

# The Waterbug Sub-Surface Sampler: Design, Control and Analysis

James Higgins and Carrick Detweiler

**Abstract**—Monitoring and predicting water quality poses significant challenges. Collecting enough information to characterize bodies of water is a critical bottleneck. Collecting data and samples from the surface all the way to the bottom over a short period of time would give water scientists the best spatio-temporal picture. In this paper, we present a small, light-weight, inexpensive water sensing and sampling robot, the “Waterbug”, capable of descending to depths up to 10m, collecting sensor information and a water sample, and returning to the surface. The water sampler also has limited capability to adjust buoyancy to hold depth for the purpose of measuring environmental conditions at specific locations in the water column. It is small enough that a single scientist could carry several in a backpack or it could be deployed by other robotic systems. The low cost of the node makes it feasible for blanket deployment. No tools are required for field servicing and the sample collection chamber is a common syringe that can be swapped quickly for redeployment. The main challenge was developing the system model and algorithm for achieving neutral buoyancy in the presence of system and initial condition variance. Over a range of conditions, we were able to achieve an 80% success rate for meeting the neutral buoyancy criteria and a 100% success rate in capturing a sample and returning to the surface.

## I. INTRODUCTION

Monitoring underwater environments plays an important role in detecting pollution, invasive species, and other environmental changes that are not apparent from terrestrial or aerial observations. Improving the type and frequency of data collection from these environments is critical for our understanding of these complex ecosystems. In-situ sensing of marine environments yields valuable insights into an aquatic habitat, but the size and expense of scientific instruments limits how much data can be collected in-situ, so physical water samples must still be collected for analysis ex-situ in offsite laboratories. Currently, collecting physical specimens is almost entirely done by hand, which is a time consuming and laborious process, and limits the spatio-temporal resolution of the environmental data.

In this paper, we present a small, inexpensive robotic sampler called the “Waterbug”, shown in Figure 1. This node is capable of collecting water samples from various depths and sensing throughout the water column. It has the ability to dive to a target depth, retrieve a sample, and ascend to the surface for retrieval using only unidirectional buoyancy

NIMBUS Lab, Dept. of Computer Science and Engineering, University of Nebraska-Lincoln, Lincoln, NE 68588, USA. {jhiggins, carrick}@cse.unl.edu.

This work was partially supported by NSF CSR-1217400, USDA #2013-67021-20947, and the Daugherty Water for Food Institute. Any opinions, findings, and conclusions or recommendations expressed in this material are those of the authors and do not necessarily reflect the views of these agencies

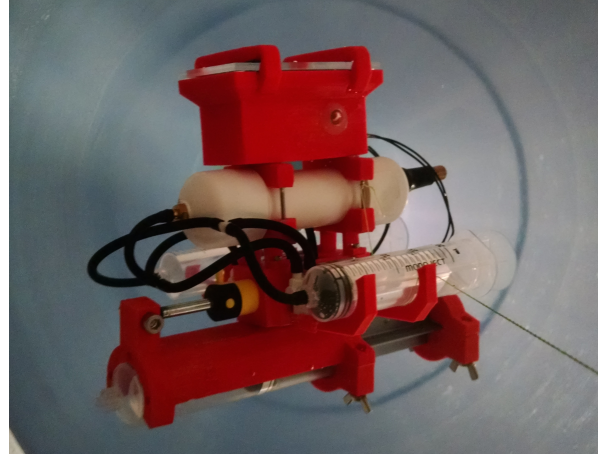


Fig. 1. Waterbug node in water during testing

control. To keep the system as simple and inexpensive as possible, we only control vertical travel since this is where the largest gradients of interest occur. In this paper, we develop a control algorithm that allows it to also achieve neutral buoyancy. These capabilities allow for ex-situ analysis of physical samples, and in-situ analysis during the deployment. A single node costs only \$120 to produce and a larger production run would cut this figure in half. This low cost and simplicity of use will allow multiple nodes to be deployed, providing high spatio-temporal resolution data.

The Waterbug was designed to only have the capability to increase buoyancy, i.e. the buoyancy controller only has unidirectional control. This eliminated half of the components from this subsystem, reducing the cost, complexity and size of the node significantly. Maintaining a small size was a design goal for the future implementation of deployment by an unmanned aerial vehicle (UAV). Only having unidirectional control necessitated an accurate mathematical model of the system and an algorithm that uses both feed-forward and feedback control to account for variance in the environment and system. Since the Waterbug has no method of adding ballast or releasing buoyancy, overshooting the buoyancy point is a failure mode from which the algorithm cannot recover. As little as 3% error in the buoyancy calculations based on initial and environmental conditions is enough to cause the node to fail to achieve neutral buoyancy according to the criteria set forth later in this work. Even with such a slight margin of error, the algorithm we developed successfully achieved neutral buoyancy in 80% of our trials and successfully captured a sample and returned to the surface in 100% of our trials for a range of initial conditions.

This paper makes the following contributions to the wa-

ter science and robotics communities. We demonstrate the effectiveness of developing an accurate system model and combining the advantages of feed-forward, feedback and precompensation to develop an algorithm that is successful despite using very inexpensive hardware. We show that it is possible to reduce cost and complexity by using only uni-directional control and still achieve similar results as other, more complex systems utilizing bi-directional control.

## II. BACKGROUND

Traditional methods of collecting water samples from depth include using Niskin bottles [1] or syringe mechanisms arranged on a string [2]. These types of methods require significant man-hours and are tedious.

Both the wireless sensor networking and robotics communities have a large body of research dedicated to underwater operation. To date, most work has considered either static sensor networks, or fully autonomous robots for monitoring water bodies. Our work combines advantages from both of these communities to create a new, more effective environmental monitoring tool.

Underwater sensor networks have a multitude of uses, including seismic monitoring, pollution detection, and environmental monitoring [3]. Most underwater sensor networks are assumed to be sparse, statically deployed networks that use expensive acoustic modems for communication [3]–[5]. Optical links for underwater communications have also been considered [6]. Traditional wireless sensor networking ideas guide these designs, which rely on many small nodes to generate and route sensor information to centralized sinks. Traditional WSNs assume that the nodes must be low cost and complexity, which reduces manufacturing and maintenance costs. The threat of water intrusion in marine environments makes this a difficult goal to achieve. Relying on underwater communication also increases cost significantly which is why we chose to not require this feature on the Waterbug and instead only require a radio to communicate at the surface.

Anchoring nodes to the seafloor with a winch allows nodes to travel vertically in the water [7], [8]. This mobility allows the nodes to find areas of interest within the water column. These nodes are expensive, and the winching mechanism consumes significant energy, which limits the deployment time and how much information is collected.

Small "drifter" nodes that float with the current of tides or rivers have been successfully deployed in the environment to take Lagrangian measurements of current but they are constrained to the surface of the water, both because they lack the actuation or buoyancy control to dive and also because their communication methods require an antenna that extends above the surface [9]–[11]. Other drifting and gliding nodes capable of descending and ascending are used to take sub-surface measurements but are more complex and expensive [12], [13].

Aquatic robots have also been used as mobile sensing platforms to study water bodies [14]–[18]. The autonomy of these robots and collaboration between them potentially resolves the difficulties of using acoustic modems and static

sensor nodes. However, these robots are large, expensive, and difficult to deploy. These shortcomings are especially difficult when working with multiple small, disconnected water bodies. In these environments it is highly desirable to avoid redeploying robots, and the number of water bodies makes it impractical to dedicate robots for every lake and pond [19]. Using small UAVs in these areas is attractive, because the high mobility allows a large area to be monitored with a small number of robots. The drawback to using UAVs is that it is extremely difficult to interact with the water, which limits the utility of their sensor data.

Small UAVs have been used to collect water samples from freshwater bodies [19], [20]. This UAV pumps water from near the surface of a water body to a reservoir in the UAV. The water samples are brought back to laboratories for detailed analysis. The small payload capacity and control complexities limit this approach to collecting small water samples from near the water's surface. The weight and complexity of a long tube make it impractical to collect water samples from deeper than a meter or two below the surface with a UAV.

## III. SYSTEM REQUIREMENTS

This section presents the high level system requirements for the Waterbug that were developed with our water science collaborators. These requirements drove the mechanical, electrical, and software design of the system.

**Size:** The system must be small enough for a scientist to carry several nodes in a backpack or for a UAV to carry and deploy a node. A Firefly hexacopter by Ascending Technologies is chosen as the reference [21]. The payload capacity of this UAV limits the total weight of the Waterbug and water sample to 600g or less. The design of the UAV attachment and deployment is outside the scope of this work, and we only consider the weight limits of the node.

**Sample Size:** A minimum of 15mL of water is needed for ex-situ analysis by limnologists [22]. The device needs to be capable of collecting and storing this amount of water. Collecting more water is beneficial, since multiple tests can then be run on each sample, or excess water can be stored for later tests.

**Collection Depth:** The Waterbug must be capable of descending to water depths of 10m, collecting a sample, and returning to the water's surface. This depth is sufficient for analyzing many freshwater rivers, lakes, and ponds, and represents a significant improvement over prior collection methods [19].

**Neutral Buoyancy:** The metric used for characterizing a successful neutral buoyancy actuation was based on a temperature sensor response time and spatial resolution. In order to get an accurate temperature reading, the node needs to hold depth for long enough that the temperature sensor has time to settle to the environment temperature. Areas of particular temperature or high temperature gradient are of interest to limnologists [23] so the ability to stop descending and observe the environment based on temperature is a significant functionality for the node. The tighter the control

over depth, the higher the resolution of the gathered data. Using a temperature sensor with a response time of 5s or less [24] as the reference for the required loiter time and a vertical resolution of approximately one length of the Waterbug yielded a functional requirement of remaining within 200mm of the target location for at least 5s.

**Field Operation:** This device will be used in remote environments by minimally trained field researchers. Therefore, the system needs to be low complexity, and not require any tools to field service. This requires the collection mechanism to be easily reset and not rely on many consumable resources so that it can be used in multiple experiments.

**Cost:** Inevitably, some nodes will be lost. The limited sensing radius of the nodes also means many will be deployed to cover an area. These factors make it important to keep the unit costs low.

#### IV. MECHANICAL DESIGN

The three main components of the mechanical system are shown in Figure 2 with the electronics pod on top removed for clarity. The pneumatic system is shown in Figure 2(a), Figure 2(b) shows the sample collection system and Figure 2(c) shows the buoyancy system. These systems are described in the subsequent sections. The mass of the complete system including a water sample is 497g. The total cost to make a single node is \$120, which is significantly less than other actuated sensor nodes and even slightly less than passive sensor nodes of similar size [9], [10]. The solenoid valves used to control the pneumatic system are the most expensive component, costing \$26 each. The overall length of the Waterbug is approximately 200mm at its greatest dimension which is important because making the node as small as possible allows better sensing of the significant vertical spatial structure in bodies of water [12]. A larger sensor or vehicle tends to have an averaging effect on these vertical structures.

**Pneumatic System:** The actuation system on the waterbug is driven by pneumatic force. The compressed air storage tank is made from 0.75in schedule 40 PVC pipe rated to withstand 480PSIG at 73.4°F and is capped with a PVC pipe cap at both ends. The internal volume of the compressed air tank is approximately  $35\text{cm}^3$ . On one end of the compressed air storage tank, a standard Schrader valve was inserted to allow charging with a standard bicycle pump or air compressor. On the other end of the tank, a barbed brass fitting was added for connecting an air line that is split with a Y-connection to run compressed air to the two solenoid valves. One solenoid valve is responsible for controlling air flow to the sample collection pneumatic piston actuators and the other solenoid valve controls air flow to the syringes used for buoyancy control. The solenoids used are ASCO™ RHB206H50B miniature two-way solenoids rated to operate at 12V and a maximum pressure of 70PSI. The solenoids draw approximately 160mA at 12V in order to open.

**Sample Collection System:** The sample collection system uses a 35mL plastic syringe to collect and store the sample. Syringes have been used by water sampling devices in

multiple research applications [2], [25], [26]. The syringes are very inexpensive which means they can be discarded after use instead of requiring time to clean for reuse. The sample collection syringe is connected to two LEGO® pneumatic actuators mounted in series. Each actuator has a stroke of 28.4mm, giving a total draw length of 56.8mm on the syringe plunger which results in 25mL of fluid collected in the syringe. The time to collect a sample is less than 2s at the maximum operational depth. The sample collection system is robust because it is completely sealed to the environment except for the inlet to the syringe where the sample is collected. This improves on other water samplers with valves open to the environment that have issues with clogging in dirty water [27]. Loosening four thumb screws releases the syringe from the two pneumatic actuators and then it snaps out of place to allow a new syringe to be snapped in place and secured to the actuators.

**Buoyancy Control System:** The Waterbug uses two 20mL syringes for one-way buoyancy control. Initially, the two buoyancy syringes are depressed so they have minimum internal volume. In this configuration, the Waterbug has a specific gravity greater than 1.0 so it sinks. After reaching the target depth or other condition, the buoyancy control solenoid is triggered to release compressed air into the two buoyancy syringes so their internal volume expands, resulting in the specific gravity of the Waterbug decreasing to less than 1.0 and it ascends to the surface for retrieval. The buoyancy syringes can also be partially expanded to achieve neutral buoyancy so that the Waterbug stops descending and maintains depth to monitor environmental conditions before collecting a sample and then fully expanding the buoyancy syringes to ascend back to the surface.

**3D Printed Parts:** The majority of the body is made from 3D printed ABS components designed using Solidworks and printed on an Ultimaker2. 3D printed parts help reduce custom part cost and since ABS can be dissolved with acetone, it is possible to make the parts waterproof by briefly dipping them in acetone to fuse the outer surface.

#### V. ELECTRICAL AND SOFTWARE DESIGN

##### A. Electrical Design

**Microcontroller:** The device uses an ATmega328P microcontroller that has 2kB of RAM, 1024bytes of EEPROM storage, 32kB of flash program memory, 8 10-bit ADCs, and 23 GPIO lines. The active power consumption is less than 12mA at the maximum clock speed, which allows the device to operate for over 48 hours with the battery used.

**Communications:** The Waterbug's main mode of communication is a 2.4GHz XBee Pro radio module that has been configured to allow remote programming of target depths. The Xbee is not intended for transmitting data while the Waterbug is submerged. Rather, it provides the convenience of interfacing with the on-board electronics and software without requiring physical access when the node is at the surface or onshore.

**Sensors:** The Waterbug currently has two main sensors on board with the capability to integrate more in the future.

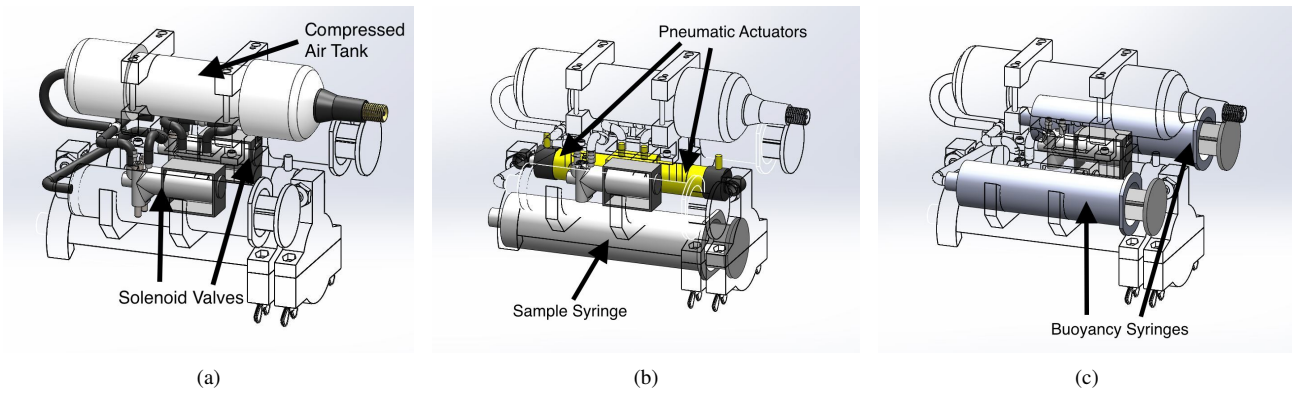


Fig. 2. (a) pneumatic system (b) sample collection system (c) buoyancy control system

The sensors currently are an absolute pressure sensor and a temperature sensor.

The pressure sensor is the most critical sensor during a deployment. This sensor enables the Waterbug to estimate its depth in the water column. The particular sensor used in the Waterbug is a Measurement Specialties MS5803-05BA. This sensor is designed for submersion and is capable of measuring from 0 – 72PSIA. The measuring end of the sensor needs to be exposed to the water but the other end of the sensor needs to be soldered to the PCB which is sealed inside the waterproof housing. A watertight seal was designed around the housing of the sensor to expose the measuring portion of the sensor while protecting the rest of the electronics from the water.

**Mechanical Actuation:** Two SSM3K329R.LF N-channel MOSFETs control the state of the solenoids that control the pneumatic actuators. The MOSFETs are rated for 3.5 amps at 30 volts which is more than sufficient for the system, which keeps them running cool despite their small footprint. The gate of each MOSFET is connected to a separate GPIO pin on the ATmega328p for independent control.

**Power:** The system is powered by a custom battery pack made from three 3.7V 750mAh single cell lithium polymer batteries connected in series.

### B. Software

For lab testing and debugging, the Waterbug can transmit data to an external receiver using the XBee radio. Currently, the sensors are polled at 80Hz for onboard calculations and data is transmitted every twentieth reading. In addition to live data transfer and flashing firmware in the lab, the XBee is used to reset the electro-mechanical components and could be used to offload data between field deployments.

## VI. CONTROL

In this section, we develop the system model and feed-forward based controller that makes up the algorithm utilized by the Waterbug to achieve neutral buoyancy with only uni-directional buoyancy control.

**Challenges, Goals, Assumptions:** One of the first challenges with this system is that the node is slow to respond to input. It takes time for the buoyancy syringes to expand after being given an input of compressed air and it takes

even more time for the node to reach a new steady state velocity after the syringes have finished expanding. This causes challenges with feedback control because system state measurements and correction attempts can be made significantly faster than the system responds which leads to overshooting and the node returning to the surface before reaching the target depth. Another challenge with feedback control stems from the mechanical nature of the syringes. Once they begin expanding, they slide quite easily, but overcoming the initial static friction takes considerably more force. Using feedback to make small corrections causes pressure to build up slowly in the buoyancy syringes and then a large jump in buoyancy when the syringes finally overcome static friction and over expand. Feedback control has the advantage of being capable of dealing with disturbance in the system but for this particular system, pure feedback is not enough to achieve the design goal.

Feed-forward control has the distinct advantage, in this case, of being capable of predicting model performance in spite of delay, but the disadvantages of requiring an accurate system model and not correcting for disturbance. For a device intended to be used in the area of field robotics, it is all but guaranteed that there will be disturbance in the system, so this must be accounted for. The goal of the controller designed for the Waterbug is to use a two stage feed-forward controller with precompensation and intermediate feedback. The precompensation and intermediate feedback adjust the controller for the possible disturbances that are measurable with the onboard sensors and that can be corrected for. The precompensation accounts for differences in the Waterbug's initial volume displacement, which can be caused by entrapped air bubbles or the buoyancy syringes not being completely depressed initially. A higher initial volume has the effect of causing the node to sink slower than expected. The second and most probable cause of deviation from the ideal model is having the starting pressure in the compressed air storage tank differ from the expected 60PSIG. The intermediate feedback accounts for this variation and is discussed in more detail later in this section.

An important assumption was made about the pressure in the syringes that would cause the mathematical model of the system to be underdetermined if not made. The pressure in

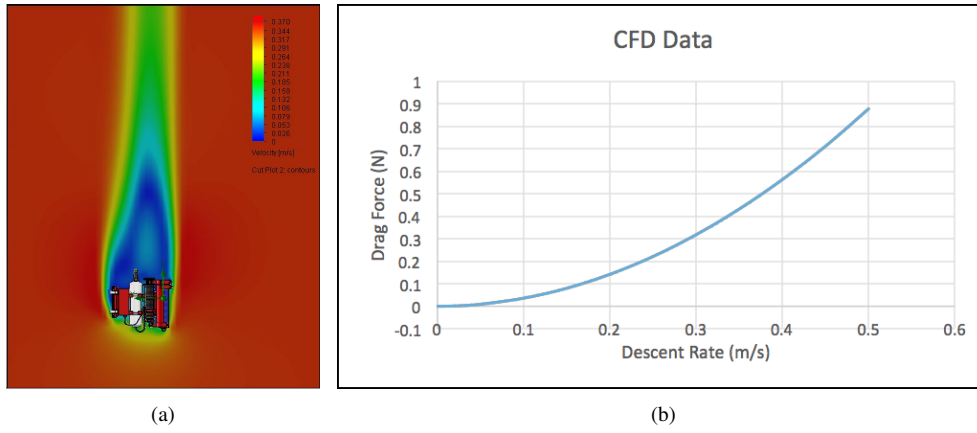


Fig. 3. (a) Section view of CFD analysis (b) Drag force vs velocity curve for CFD data combined with validation tests

the syringes is assumed to be equal to the external pressure from depth as long as the syringes haven't fully expanded. Once the syringes have fully extended and reached their stops, the internal pressure will increase beyond the external pressure, but at this point, additional input from the controller yields no increase in buoyancy, so it is outside the region governed by the controller. The assumption is reasonable because the syringes slide quite easily once they begin to expand so the plunger will continue expanding until the internal compressed air pressure approximately equals the external water pressure. The friction has a damping effect that contributes to the delay in the system but the magnitude of the force is negligible when compared to the force from pressure at depth.

The Waterbug is designed so that the center of buoyancy is offset from the center of gravity. This ensures that it sinks in the same orientation for consistent performance.

**Computational Fluid Dynamics (CFD) Analysis:** The Solidworks Flow Simulation package was used to estimate the steady state drag force on the Waterbug during descent. This information was needed to help design the feed-forward control. Figure 3(a) shows the velocity profile of water flowing around the Waterbug, the boundary layer that develops ahead and the wake that forms behind. The areas of lowest velocity correspond to the highest drag. The analysis computed the total drag force on the Waterbug for a given input velocity. The force was computed for descent rates increasing by 0.05 m/s increments starting from 0 m/s. This data was used to generate the graph shown in Figure 3(b) which shows the descent rate vs steady state force.

Physical validation tests were performed and the CFD and physical sets of data were compared to yield the equation,

$$F_d = 7.4498v^2 - 0.0926v - 0.0027 \quad (1)$$

where  $F_d$  is the drag force and  $v$  is the descent rate. Using the calculated descent rate and the previous function, the steady state drag force can be calculated during an actual descent. Since the drag force is equal to the buoyancy force once steady state conditions have been reached, the previous relationship between descent rate and drag force allows direct correlation between descent rate and buoyancy conditions,

which allows a mathematical model to be developed from knowledge of the descent rate.

**Mathematical Model:** The goal of the model is to find the required time necessary to open the solenoid valve in order to achieve a desired descent velocity.

The buoyancy force is given by the equation

$$B_F = V_{wb}\rho_w g - m_{wb}g \quad (2)$$

where  $B_F$  is the buoyancy force,  $m_{wb}$  is the mass of the Waterbug,  $V_{wb}$  is the volume displaced by the Waterbug,  $\rho_w$  is the density of water and  $g$  is the acceleration due to gravity. The mass of the Waterbug, the density of water and the acceleration due to gravity are all known quantities. Since the steady state drag force can be calculated from the descent rate using equation (1), the only unknown remaining in equation (2) is the time varying volume of the Waterbug.

Applying Boyle's law [28] yields the equation

$$P_{t1}V_t = P_t V_t + P_{syr}V_{syr} \quad (3)$$

where  $P_{t1}$  is the initial pressure in the compressed air storage tank and  $V_t$  is the fixed volume of the compressed air storage tank.  $P_t$  is the time varying pressure in the compressed air storage tank.  $P_{syr}$  and  $V_{syr}$  are the pressure and volume in the buoyancy syringes. The product on the left hand side of equation (3) is constant and the pressure in the syringes is approximately equal to the pressure from depth during the times considered which is given by the following equation

$$P_{syr} = \rho_w g h + P_{atm} \quad (4)$$

where  $h$  is the depth below the surface of the water and  $P_{atm}$  is the atmospheric pressure.

The time varying pressure in the compressed air storage tank is modeled as a linear, first order ODE, shown in equation (5).

$$P_t = Ae^{-Bt_{open}} + P_f \quad (5)$$

The constant  $P_f$  at the end of equation (5) is the final pressure in the tank as time goes to infinity. Using initial conditions and internal volumes,  $A$  can be solved for:  $A = 0.532 * P_{t1}$ . Rearranging equation (3) with the new form for  $P_t$  and solving for the total node volume yields,

$$V_{wb} = V_c + \frac{P_{t1}V_t - V_t(0.532 * P_{t1}e^{-Bt_{open}} + P_f)}{P_{syr}(t)} \quad (6)$$

where  $V_c$  is the Waterbug volume when the buoyancy syringes are compressed and  $t_{open}$  refers to the amount of time the buoyancy solenoid valve has been open. The compressed volume of the Waterbug is approximately  $450cm^3$ . Plugging equation (6) into equation (2) and solving for  $t_{open}$  gives,

$$t_{open} = \frac{\ln \frac{0.532 - \left( \frac{m_{wb}g - (7.4498v^2 - 0.0926v - 0.0027)}{\rho_{wg}} - V_c \right) \frac{P_{syr}}{P_{t1}V_{t1}}}{0.532}}{-B}}{\quad} \quad (7)$$

which is a fully parametric equation solving for the time the solenoid valve needs to open for a given pressure in the compressed air tank, target descent velocity, depth, node volume, mass and appropriate coefficient  $B$ . Under the assumptions that the compressed air tank starts at a known pressure, the Waterbug volume and mass are known and the pressure, i.e. depth, can be measured using the onboard pressure sensor, the only unknown in equation (7) is the coefficient,  $B$ . The appropriate value for  $B$  was empirically solved for by carefully controlling the starting pressure in the tank so that the only variable in the model was  $B$  and then performing iterative trials with different values until the mathematical model corresponded with the physical tests.

## VII. NEUTRAL BUOYANCY ALGORITHM

Algorithm 1 shows an overview of the flow of the control algorithm. After the node is released at the surface, the descent rate is measured in line 3 after reaching a steady state and the model is precompensated to account for the true starting volume, which cascades through the algorithm. Steady state velocity must be achieved first so that the drag force is equal to the buoyancy force which allows equation (1) to be substituted into equation (2) and the actual Waterbug volume to be calculated based on the measured descent velocity.

$$V_c = \frac{(7.4498v^2 - 0.0926v - 0.0027) + m_{wb}g}{\rho_{wg}} \quad (8)$$

The next stage of the controller is feed-forward for the purpose of calibration. Equation (7) is utilized in line 7 to find the required time to open the solenoid valve, with an assumed starting pressure of 60PSIG in the tank, in order to slow to one quarter terminal velocity of the fully compressed node, i.e. 50mm/s. The actual descent velocity of the Waterbug is measured in line 10 after pulsing the solenoid for the calculated time and waiting until the new steady state velocity is achieved. The projected target velocity of 50mm/s is based on an assumed starting pressure in the tank. The actual measured velocity is used to correct the assumption and back calculate the true initial pressure by rearranging equation (7) and solving for  $P_{t1}$ .

$$P_{t1} = \frac{\left( \frac{m_{wb}g - (7.4498v^2 - 0.0926v - 0.0027)}{\rho_{wg}} - V_c \right) P_{syr}}{V_t(0.532 - 0.532e^{-Bt_{open}})} \quad (9)$$

If the true pressure is not sufficient to expand the syringes at the target depth, the node can abort and return to the surface. Once the true starting pressure is calculated and determined sufficient, the variances that can be accounted for in the model are known and the new values can be used to calculate the total time necessary to open the solenoid valve to achieve zero velocity at the target depth shown in line 17. Once this depth is reached, the solenoid valve is opened for the calculated time minus the time already opened during the calibration stage. The Waterbug delays at least 5 seconds, then collects a sample and returns to the surface shown in lines 19 – 21.

```

1: procedure NEUTRALBUOYANCY&SAMPLING()
2:   if steady state velocity achieved then
3:     measureVelocity()
4:     //use true volume to precompensate controller
5:     calcTrueVolume()           ▷ use equation 8
6:     //target v=50mm/s
7:     calibPulse()             ▷ use equation 7
8:   end if
9:   if new steady state velocity achieved then
10:    measureVelocity()
11:    //back calculate true starting pressure
12:    calcTruePressure()       ▷ use equation 9
13:  end if
14:  //wait until target depth is achieved
15:  if target depth achieved then
16:    //target v=0mm/s
17:    calcOpenTime()           ▷ use equation 7
18:    solenoidOn = calcOpenTime - calibPulse
19:    delay(5s+)
20:    collectSample()
21:    returnToSurface()
22:  end if
23: end procedure

```

Algorithm 1: Neutral Buoyancy and Sampling Algorithm

## VIII. EVALUATION

A series of tests evaluated the mechanical and electrical performance of the system. These tests reveal the capabilities of the system, and point towards future improvements to be made so that the device is field operable.

**Maximum Depth Test:** In order to test the maximum functional depth of the Waterbug, a pressure vessel was used to simulate the pressure that would be experienced. This allowed easy visibility and recovery when the maximum functional depth was exceeded. Initially, 10m depth was simulated by pressurizing the vessel to 14.2PSIG with the node inside and triggering a sample sequence. The Waterbug performed a complete cycle that would have resulted in a full sample being collected and then ascending to the



Fig. 4. 10ft vertical water column for in-water lab testing

surface which verified that the node achieved its design parameter. For the sake of completeness, subsequent tests were performed to determine how deep the Waterbug could go and still be able to ascend to the surface.

At a simulated depth of 11.2m in the pressure vessel, the Waterbug just barely collected a full sample and fully expanded the buoyancy syringes. However, the buoyancy syringes required 10s to expand and since the node will continue to descend until the syringes have almost fully expanded, it likely would not have completed the expansion as pressure continued to increase with depth in a real scenario. Therefore, 11m is considered the cutoff depth for being capable of returning to the surface.

**Neutral Buoyancy Control:** A test apparatus shown in Figure 4 was constructed from a 10' long, 12" diameter clear PVC tube stood on end and filled with water. This allowed for moderate depth tests while being able to maintain good visibility of the node for evaluation, which is not possible in a pool or lake.

As stated earlier, the minimum criteria for a successful neutral buoyancy actuation is maintaining depth within one body length, i.e. 200mm, of the target location for at least 5s to allow settling time for a temperature sensor to get an accurate reading. 35 successive trials were performed to evaluate the performance of the system and control algorithm over three ranges of initial conditions shown in Table I. Over the 35 trials, the Waterbug had an overall success rate of 80% for maintaining depth within 200mm of the target location for at least 5s and a 100% success rate for collecting a sample and returning to the surface. Of the trials that failed to achieve neutral buoyancy, 5 trials overshot the buoyancy point and 2 undershot. The trials that undershot did not slow their descent enough to stay in the target zone for the required time and the trials that overshot became too buoyant and

Starting Pressure (PSI)	Trials	Success (%)	Mean Dwell (s)
55-59	10	90	16.6
60-64	15	73	15.3
65-70	10	80	10.8

TABLE I  
RESULTS OF NEUTRAL BUOYANCY ATTEMPTS

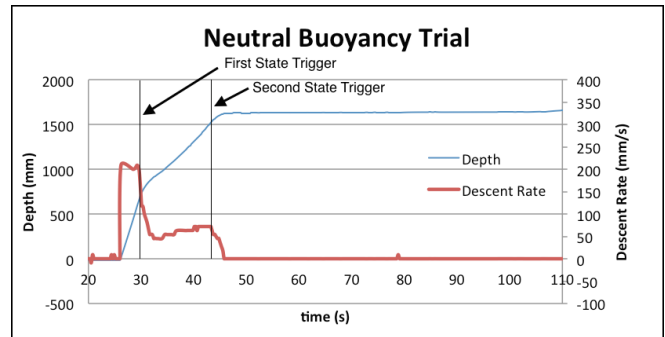


Fig. 5. depth and descent rate data for a neutral buoyancy trial

ascended out of the target zone before 5s elapsed.

Figure 5 shows a plot of the depth and descent rate for one of the successful trial experiments. When the Waterbug reaches a depth of 600mm, the calibration stage is triggered, which slows the node to just over 70mm/s. This means that the true starting pressure in the tank was under the assumed 60PSIG. At the target depth of 1500mm, the second stage triggers and the node becomes neutrally buoyant and settles around 1630mm.

Mechanical inconsistencies and initial conditions too far outside the working envelope were the cause of the Waterbug failing to remain within 200mm of the target location for at least 5s after a neutral buoyancy attempt. At a starting pressure of 75PSIG in the compressed air tank, the first calibration stage of the control algorithm intended to only slow the descent caused the Waterbug to actually become positively buoyant and return to the surface before the rest of the algorithm could even run. Therefore, this bounded the upper limit for the initial conditions. The lower limit is bounded by the required pressure to return to the surface from a given depth.

The trials within the functional bounds that failed were caused by the buoyancy syringes expanding an inconsistent amount. Even when given identical input, the expansion output would occasionally differ from the expected amount. The suspected cause of this problem is inconsistent friction in the buoyancy syringes. This problem is difficult to mitigate because the system model cannot account for this disturbance. Using feedback to correct for it is also challenging because the delay between input correction and output change is large and overshooting produces immediate failure because the controller only has uni-directional control.

## IX. FUTURE WORK AND CONCLUSIONS

The main source of failure in the neutral buoyancy algorithm stemmed from mechanical inconsistency of the buoyancy syringes. Finding a suitable lubricant to grease the seals on the syringe may help by reducing the friction

between the seal and body to provide more consistent results. It is also possible that such an inexpensively manufactured component could have slight dimensional or surface finish variations and one syringe may perform better than another. Selectively taking the best syringes from a sample set may improve the success rate of the neutral buoyancy algorithm. In summary, more investigation needs to be performed to find a suitable solution for this particular issue.

In addition, we plan to conduct field tests, because inevitably, nature finds ways of exposing weaknesses in design that the lab environment never can. The Waterbug will be used to collect actual water samples and these samples will need to be compared to samples collected through traditional means to make sure the Waterbug does not ruin the fidelity of the samples.

We also plan to integrate the Waterbug with a UAV for deployment and retrieval. The significant challenge with this will be localizing the Waterbug with the UAV and reattaching for return to the shore.

In conclusion, the Waterbug satisfies its design goals of being inexpensive, small in size, light enough to be carried by a UAV, and being capable of descending to 10m, collecting a sample and ascending to the surface. It also successfully achieved neutral buoyancy 80% of the time over a range of parameters simulating field conditions. We demonstrated the effectiveness of developing an accurate system model and combining the advantages of feed-forward, feedback and precompensation to develop an algorithm that is successful despite using very inexpensive hardware. We showed that it is possible to reduce cost and complexity by using only uni-directional control and still achieve similar results as other, more complex systems utilizing bi-directional control.

#### X. ACKNOWLEDGMENTS

Thank you to David Anthony, John-Paul Ore and Ajay Shankar of the NIMBUS lab for their help with electronics design and prototyping as well as editorial input.

#### REFERENCES

- [1] N. J., "Water sampler device," Jan. 13 1970, uS Patent 3,489,012. [Online]. Available: <https://www.google.com/patents/US3489012>
- [2] I. A. Blakar, "A close-interval water sampler with minimal disturbance properties," *Limnology and Oceanography*, vol. 24, no. 5, pp. 983–988, 1979.
- [3] I. F. Akyildiz, D. Pompili, and T. Melodia, "Underwater acoustic sensor networks: research challenges," *Ad Hoc Networks*, vol. 3, no. 3, pp. 257–279, May 2005.
- [4] K. Akkaya and A. Newell, "Self-deployment of sensors for maximized coverage in underwater acoustic sensor networks," *Comput. Commun.*, vol. 32, no. 7-10, pp. 1233–1244, May 2009.
- [5] I. Vasilescu, C. Detweiler, and D. Rus, "AquaNodes: An underwater sensor network," in *Proceedings of the Second Workshop on Underwater Networks*, ser. WUWNet '07. New York, NY, USA: ACM, 2007, pp. 85–88.
- [6] M. Doniec, I. Vasilescu, M. Chitre, C. Detweiler, M. Hoffmann-Kuhnt, and D. Rus, "Aquaoptical: A lightweight device for high-rate long-range underwater point-to-point communication," in *OCEANS 2009, MTS/IEEE Biloxi - Marine Technology for Our Future: Global and Local Challenges*, Oct 2009, pp. 1–6.
- [7] C. Detweiler, M. Doniec, M. Jiang, M. Schwager, R. Chen, and D. Rus, "Adaptive decentralized control of underwater sensor networks for modeling underwater phenomena," in *Proceedings of the 8th ACM Conference on Embedded Networked Sensor Systems*, ser. SenSys '10. New York, NY, USA: ACM, 2010, pp. 253–266.

- [8] C. Detweiler, M. Doniec, I. Vasilescu, E. Basha, and D. Rus, "Autonomous depth adjustment for underwater sensor networks," in *Proceedings of the Fifth ACM International Workshop on Underwater Networks*, ser. WUWNet '10. New York, NY, USA: ACM, 2010, pp. 12:1–12:4.
- [9] A. Tinka, Q. Wu, K. Weekly, C. A. Oroza, J. Beard, and A. M. Bayen, "Heterogeneous fleets of active and passive floating sensors for river studies," *Journal of Field Robotics*, 2015.
- [10] J. Austin and S. Atkinson, "The design and testing of small, low-cost gps-tracked surface drifters," *Estuaries*, vol. 27, no. 6, pp. 1026–1029, 2004.
- [11] J. Beard, K. Weekly, C. Oroza, A. Tinka, and A. M. Bayen, "Mobile phone based drifting lagrangian flow sensors," in *Networked Embedded Systems for Every Application (NESEA), 2012 IEEE 3rd International Conference on*. IEEE, 2012, pp. 1–7.
- [12] J. Jaffe and C. Schurgers, "Sensor networks of freely drifting autonomous underwater explorers," in *Proceedings of the 1st ACM international workshop on Underwater networks*. ACM, 2006, pp. 93–96.
- [13] R. E. Davis, C. C. Eriksen, and C. P. Jones, "Autonomous buoyancy-driven underwater gliders," pp. 37–58, 2002.
- [14] H. Singh, A. Can, R. Eustice, S. Lerner, N. McPhee, O. Pizarro, and C. Roman, "Seabed AUV offers new platform for high-resolution imaging," *Eos, Transactions American Geophysical Union*, vol. 85, no. 31, pp. 289–296, 2004.
- [15] G. Dudek, P. Giguere, C. Prahacs, S. Saunderson, J. Sattar, L. A. Torres-Mendez, M. Jenkin, A. German, A. Hogue, A. Ripsman, and others, "Aqua: An amphibious autonomous robot," *IEEE Computer*, vol. 40, no. 1, pp. 46–53, 2007.
- [16] R. Camilli, B. Bingham, M. Jakuba, H. Singh, and J. Whelan, "Integrating in-situ chemical sampling with AUV control systems," in *OCEANS'04. MTS/IEEE TECHNO-OCEAN'04*, vol. 1. IEEE, 2004, pp. 101–109.
- [17] B. Allen, R. Stokey, T. Austin, N. Forrester, R. Goldsborough, M. Purcell, and C. von Alt, "REMUS: a small, low cost AUV; system description, field trials and performance results," in *OCEANS'97. MTS/IEEE Conference Proceedings*, vol. 2. IEEE, 1997, pp. 994–1000.
- [18] A. Lucieer, D. Turner, D. H. King, and S. A. Robinson, "Using an unmanned aerial vehicle (UAV) to capture micro-topography of antarctic moss beds," *International Journal of Applied Earth Observation and Geoinformation*, vol. 27, pp. 53–62, 2014.
- [19] J.-P. Ore, S. Elbaum, A. Burgin, B. Zhao, and C. Detweiler, "Autonomous aerial water sampling," in *Proc. of The 9th Intl. Conf. on Field and Service Robots (FSR)*. Brisbane, Australia, vol. 5, 2013.
- [20] J.-P. Ore, S. Elbaum, A. Burgin, and C. Detweiler, "Autonomous aerial water sampling," *Journal of Field Robotics*, vol. 32, no. 8, pp. 1095–1113, 2015.
- [21] "Ascending Technologies." [Online]. Available: <http://www.ascotec.de>
- [22] A. D. Eaton and M. A. H. Franson, *Standard methods for the examination of water & wastewater*. American Public Health Association, 2005.
- [23] M. Chung, C. Detweiler, M. Hamilton, J. Higgins, J.-P. Ore, and S. Thompson, "Obtaining the thermal structure of lakes from the air," *Water*, vol. 7, no. 11, p. 6467, 2015. [Online]. Available: <http://www.mdpi.com/2073-4441/7/11/6467>
- [24] B. Garnier and F. Lanzetta, "Tutorial 4: In situ realization/characterization of temperature/heat flux sensors," Technical Report, Tech. Rep., 2011.
- [25] J. B. Martin, R. G. Thomas, and K. M. Hartl, "An inexpensive, automatic, submersible water sampler," *Limnology and Oceanography: Methods*, vol. 2, no. 12, pp. 398–405, 2004.
- [26] L. E. Bird, A. Sherman, and J. Ryan, "Development of an active, large volume, discrete seawater sampler for autonomous underwater vehicles," in *OCEANS 2007*. IEEE, 2007, pp. 1–5.
- [27] A. Marouchos, C. Neill, M. Sherlock, T. Goodwin, E. Van Ooijen, J. Cordell, and B. Tilbrook, "Challenges in autonomous coastal water sampling," in *Oceans, 2012*. IEEE, 2012, pp. 1–6.
- [28] "Boyle's law." [Online]. Available: [//www.oxfordreference.com/10.1093/acref/9780199233991.001.0001/acref-9780199233991-e-325](http://www.oxfordreference.com/10.1093/acref/9780199233991.001.0001/acref-9780199233991-e-325)